The Transcriptional Regulator LEUNIG_HOMOLOG Regulates Mucilage Release from the Arabidopsis Testa[1][W][OA]

Murray Walker[2], Muhammad Tehseen[2,3], Monika S. Doblin, Filomena A. Pettolino[4], Sarah M. Wilson, Antony Bacic, and John F. Golz*

Genetics Department (M.W., M.T., J.F.G.), Plant Cell Biology Research Centre, School of Botany (M.S.D., F.A.P., S.M.W., A.B.), and Australian Research Council Centre of Excellence in Plant Cell Walls, School of Botany (M.S.D., S.M.W., A.B.), University of Melbourne, Victoria 3010, Australia

Exposure of the mature Arabidopsis (*Arabidopsis thaliana*) seed to water results in the rapid release of pectinaceous mucilage from the outer cells of the testa. Once released, mucilage completely envelops the seed in a gel-like capsule. The physical force required to rupture the outer cell wall of the testa comes from the swelling of the mucilage as it expands rapidly following hydration. In this study, we show that mutations in the transcriptional regulator *LEUNIG_HOMOLOG* (*LUH*) cause a mucilage extrusion defect due to altered mucilage swelling. Based on sugar linkage and immunomicroscopic analyses, we show that the structure of *luh* mucilage is altered, having both an increase in substituted rhamnogalacturonan I and in methyl-esterified homogalacturonan. Also correlated with the structural modification of *luh* mucilage is a significant decrease in *MUCILAGE MODIFIED2* (*MUM2*; a β-galactosidase) expression in the *luh* seed coat, raising the possibility that reduced activity of this glycosidase is directly responsible for the *luh* mucilage defects. Consistent with this is the structural similarity between *mum2* and *luh* mucilage as well as the observation that elevating *MUM2* expression in *luh* mutants completely suppresses the mucilage extrusion defect. Suppression of the *luh* mutant phenotype was also observed when LEUNIG, a transcriptional corepressor closely related to LUH, was introduced in *luh* mutants under the control of the *LUH* promoter. Based on these data, we propose a new model for the regulation of pectin biosynthesis during plant growth and development.

Seed development in angiosperms is characterized by the formation of the embryo, endosperm, and seed coat. Unlike the embryo and endosperm, the seed coat is derived from the ovule integuments and therefore is of maternal origin. Seed coat differentiation is characterized by extensive modifications of integument cells that in many species involve the formation of thickened cell walls followed by cell death. These specialized cell layers protect the embryo from dehydration, physical damage, and pathogen attack as well as playing important roles in controlling dormancy, germination, and seed dispersal (Leon-Kloosterziel et al., 1994; Boesewinkel and Bouman, 1995).

In myxospermous species such as Arabidopsis (*Arabidopsis thaliana*), cells in the outer layer of the seed coat (testa) synthesize and secrete large quantities of mucilage into the apoplast between the radial and outer tangential cell walls (Beeckman et al., 2000; Western et al., 2000; Windsor et al., 2000). During the differentiation process, the internal structure of mucilage-secreting cells (MSC) also changes dramatically. Initially, vacuolar expansion drives the growth of MSC, but this is soon followed by a rapid reduction in vacuole volume as the cells begin to secrete mucilage into the apoplast. Accumulating mucilage eventually forces the cytoplasm into the center of the cell, where it forms a column. The last stages of MSC differentiation are characterized by the thickening of the radial cell walls and extensive deposition of cell wall material into the cytoplasmic column, resulting in its conversion into a volcano-shaped columella. Finally, as the seed becomes progressively desiccated, the MSC collapse, leaving a ring of dehydrated mucilage around the base of the columella. When the mature seed is next exposed to water following dispersal, mucilage swells rapidly, causing the rupture of the MSC. Released

[1] This work was supported by the University of Melbourne (start-up grant to J.F.G.), the Australian Research Council Centre of Excellence in Plant Cell Walls and a linkage project grant, and the Commonwealth Scientific and Research Organisation Flagship Collaborative Research Program, provided to the High Fibre Grains Cluster via the Food Futures Flagship (to A.B.).

[2] These authors contributed equally to the article.

[3] Present address: Commonwealth Scientific and Industrial Research Organization Ecosystems Sciences, Clunies Ross St., Black Mountain, Canberra, ACT 2601, Australia.

[4] Present address: Commonwealth Scientific and Industrial Research Organization Plant Industry, GPO Box 1600, Canberra, ACT 2601, Australia.

* Corresponding author; e-mail jgolz@unimelb.edu.au.

The author responsible for distribution of materials integral to the findings presented in this article in accordance with the policy described in the Instructions for Authors (www.plantphysiol.org) is: John F. Golz (jgolz@unimelb.edu.au).

[W] The online version of this article contains Web-only data.

[OA] Open Access articles can be viewed online without a subscription.

www.plantphysiol.org/cgi/doi/10.1104/pp.111.172692

mucilage subsequently envelops the seed in a gelatinous gel (Western et al., 2000). While the function of seed mucilage is not well understood, suggested roles include aiding seed dispersal, protecting the germinating seed against dehydration, and, in some species, maintaining seed viability in harsh environments (Gutterman and Shemtov, 1996; Penfield et al., 2001).

Treating imbibed Arabidopsis seeds with ruthenium red, a dye that binds to carboxyl groups typical of acidic pectic polysaccharides, reveals two distinct layers of mucilage (Western et al., 2000, 2001). The outer layer is diffuse, stains poorly with ruthenium red, and is easily detached from the seed by agitation. Due to the ease of extraction, this layer is often referred to as the water-soluble layer. In contrast, the inner adherent layer directly adjacent to the testa stains more intensely with ruthenium red and cannot be easily detached from the seed. Structural analysis of the water-soluble mucilage layer has shown that it is primarily composed of unsubstituted rhamnogalacturonan I (RG-I), a pectin with an alternating α-1,4-linked GalUA (GalA) and α-1,2-linked Rha residue backbone (Western et al., 2000, 2004; Penfield et al., 2001; Usadel et al., 2004; Macquet et al., 2007a, 2007b). Use of more vigorous extraction methods also identified RG-I as the major pectin of the inner mucilage layer, although in this case, the presence of arabinans and (arabino)galactans suggests that this pectin is more highly substituted than its counterpart in the outer layer (Macquet et al., 2007a). Homogalacturonan (HG) represents only a small fraction of the pectin present in Arabidopsis mucilage and is mostly located within the inner adherent layer (Macquet et al., 2007a). The distribution of HG is not homogeneous, as highly methyl esterified HG is confined to the periphery of the inner layer while sparsely methyl esterified HG is found located in dense patches above the columella (Macquet et al., 2007a). Furthermore, the presence of cellulose in the inner domain of the inner adherent layer is thought to play a role in tethering mucilage to the seed coat (Macquet et al., 2007a).

Analysis of mutants has identified two groups of genes required for normal mucilage extrusion from the Arabidopsis seed coat. The first is a series of transcription factors, APETALA2, ENHANCER OF GLABRA3 (EGL3), GLABRA2 (GL2), MYB PROTEIN5 (MYB5), MYB61, TRANSPARENT TESTA8 (TT8), TRANSPARENT TESTA GLABRA1 (TTG1), and TTG2, that promote seed coat differentiation and hence mucilage biosynthesis as well as regulating a range of other developmental processes (Koornneef, 1981; Bowman et al., 1989; Nesi et al., 2000; Penfield et al., 2001; Western et al., 2001, 2004; Johnson et al., 2002; Zhang et al., 2003; Li et al., 2009). The second group of genes, called *MUCILAGE MODIFIED (MUM)*, specifically affect the amount and/or structure of mucilage, having little or no effect on seed coat differentiation (Western et al., 2001). Of these, *RHAMNOSE SYNTHASE2* (*RHM2*)/*MUM4* encodes an enzyme involved in the synthesis of UDP-L-Rha, which presumably supplies most of the Rha required for RG-I synthesis in the mucilage-secreting cells of the testa (Usadel et al., 2004; Western et al., 2004; Oka et al., 2007). In addition to altering the quantity of mucilage, *mum4* is the only mutant in this class to display overt columella defects, suggesting a link between pectin biosynthesis and cell wall thickening (Western et al., 2004). Although *mum2* mutants fail to release mucilage when hydrated, chemically weakening the cell wall of the seed induces a small amount of mucilage extrusion (Western et al., 2004). However, *mum2* mucilage expands poorly, indicating likely structural modifications that affect mucilage hydration. Consistent with a role in regulating mucilage structure, *MUM2* encodes a β-galactosidase that removes galactosyl residues from the galactan side chains present on the RG-I backbone following secretion into the apoplast (Dean et al., 2007; Macquet et al., 2007b).

While not identified as a *mum* mutant, loss of bifunctional β-D-xylosidase/α-L-arabinofuranosidase (BXL1) activity also affects mucilage structure by increasing the proportion of α-1,5-L-arabinan (Ara) attached to the RG-I backbone (Arsovski et al., 2009). In this case, elevated RG-I substitution is associated with a slow and patchy release of mucilage from the seed following hydration (Arsovski et al., 2009). Another recent study has shown that mutations in *GAUT11*, a putative galacturonosyltransferase involved in RG-I biosynthesis, also affect the quantity and hydration properties of mucilage (Caffall et al., 2009). Interestingly, not all mucilage-deficient mutants have defects in RG-I structure. Mutations in the subtilisin-like Ser protease *AtSBT1.7* are associated with a significant reduction in HG methyl esterification, which not only affects mucilage release from the seed but also changes the viscosity of the outer cell wall of the testa (Rautengarten et al., 2008).

Given the structural complexity of pectin, it is assumed that a large number of glycosyltransferases, sugar nucleotide-interconverting enzymes, methyltransferases, and acetyltransferases are involved in pectin biosynthesis. While recent progress has seen some of these enzymes identified (for review, see Mohnen, 2008), almost nothing is known about the molecular mechanisms regulating these biosynthetic pathways. Here, we present a detailed characterization of the mucilage extrusion defects associated with mutations in the transcriptional regulator LEUNIG_HOMOLOG (LUH). Using biochemical analysis, we show that the RG-I present in *luh* mucilage is more substituted than RG-I from wild-type mucilage and that this is associated with an increased proportion of terminal Gal residues attached to the RG-I backbone. We show that *LUH* is allelic to *MUM1*, and the β-galactosidase *MUM2* is a likely target of *LUH* regulation. Finally, we present evidence that the transcriptional corepressor LEUNIG (LUG) is functionally interchangeable with LUH, raising the possibility that LUH functions as a repressor during seed coat maturation. We propose that LUH controls *MUM2* activity

indirectly via an as yet unidentified MUM2 negative regulator.

RESULTS

luh Mutants Display a Mucilage Extrusion Defect Associated with Altered Mucilage Hydration Properties

A characteristic feature of *luh* mutants is delayed germination when plated onto Murashige and Skoog medium (Sitaraman et al., 2008). As previous work has established a link between mucilage release (extrusion) and germination (Arsovski et al., 2009), we examined whether *luh* seeds release mucilage normally. When hydrated wild-type seeds are treated with the dye ruthenium red, released mucilage appears as a red halo around the seed (Fig. 1A) and the volcano-shaped columellae become more prominent due to rupture of the MSC (Fig. 1B). Absence of a ruthenium red halo surrounding imbibed *luh* seeds, together with a lack of distinguishable columellae (Fig. 1, C and D), indicate that the MSC fail to rupture when exposed to water.

Possible reasons for this extrusion defect include disruptions to seed coat differentiation, reductions in mucilage biosynthesis, or alterations to mucilage fine structure (Western et al., 2001, 2004; Dean et al., 2007; Macquet et al., 2007b). Because the first two defects are associated with altered MSC morphology, we used scanning electron microscopy (SEM) to examine the surface of *luh* seeds. Like the wild type, *luh* MSC had a hexagonal appearance with thick radial cell walls and a central columella (Fig. 1, E and F). A depression in the center of the columella was frequently observed in the strong *luh-1* mutant (Fig. 1F, arrowheads) but was not a consistent feature of other *luh* alleles (Supplemental Fig. S1). Likewise, comparisons of histological sections through wild-type and *luh* MSC revealed few differences. At 6 d post anthesis (dpa), numerous amyloplasts were visible in the cytoplasm of both wild-type and *luh* cells, together with mucilage accumulation in the apoplastic space (Fig. 1, G and H). By 9 dpa, the cytoplasm of wild-type and *luh* cells was confined to a central column, in both cases exhibited cell wall thickening. This process was slightly more advanced in *luh* mutants, as cytoplasmic disintegration was apparent (Fig. 1, I and J). Formation of the columella was complete in 12-dpa *luh* seeds but was not as advanced in wild-type cells (Fig. 1, K and L). Despite the apparent acceleration of *luh* seed coat maturation, there was no obvious difference in the amount of pink-staining mucilage material seen in wild-type and *luh* MSC.

Absence of patterning or mucilage secretion defects in *luh* mutants led us to consider whether the hydration properties of *luh* mucilage were altered. To test this, we first weakened the outer seed coat cell wall by gently shaking seeds in a solution of weak alkali (1 M

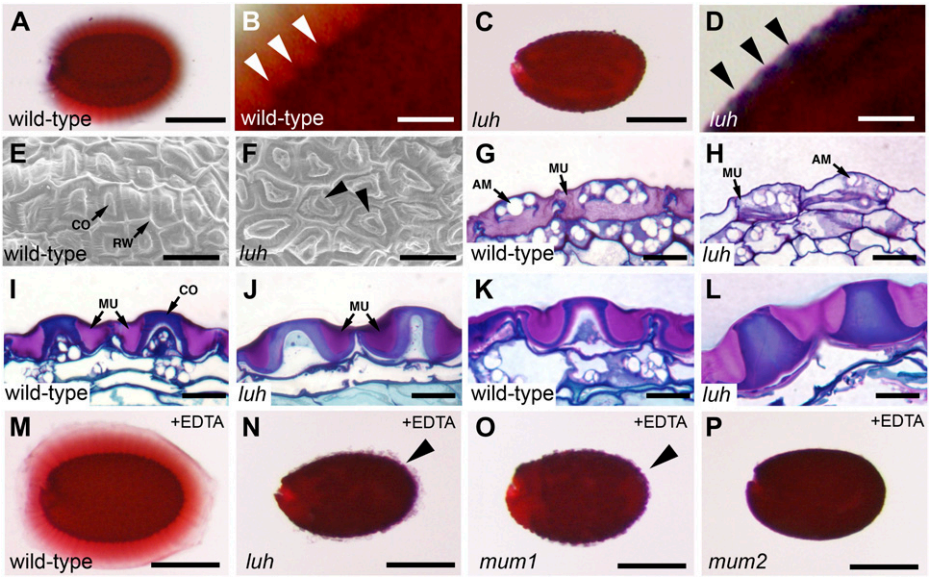

Figure 1. Structure and development of wild-type and *luh* mutant seed coats. A and B, Ruthenium red-stained mature wild-type seed (A) and close-up view of columellae (white arrowheads) protruding from the seed surface (B). C and D, Ruthenium red-stained *luh-4* seed (C) and view of enclosed columellae (black arrowheads) within the MSC of the testa (D). E and F, Scanning electron micrographs showing the surface morphology of wild-type (E) and *luh-1* (F) MSC. Arrowheads in F indicate abnormal doughnut-shaped columellae. G to L, Longitudinal sections through wild-type (G, I, and K) and *luh-4* mutant (H, J, and L) seeds at 6 dpa (G and H), 9 dpa (I and J), and 12 dpa (K and L) stained with toluidine blue. M to P, Ruthenium red-stained seeds from wild-type (M), *luh-4* (N), *mum1-1* (O), and *mum2-1* (P) plants following a 2-h treatment with 50 mM EDTA. Arrowheads indicate small amounts of mucilage release from *luh* and *mum1* mutants. AM, Amyloplasts; CO, columella; MU, mucilage; RW, radial wall. Bars = 250 μm in A, C, and M to P and 50 μm in B, D, and E to L.

Na_2CO_3), a mild cation chelator (0.2% [w/v] ammonium oxalate), or a strong cation chelator (50 mM EDTA) for 2 h before staining with ruthenium red. All three treatments caused a small amount of mucilage release, with EDTA having the greatest effect (Fig. 1N; Supplemental Fig. S2). Interestingly, released *luh* mucilage did not expand properly and stained poorly with ruthenium red (Fig. 1, compare M and N). These observations indicate that the hydration properties of *luh* mucilage have been significantly altered. This phenotype is shared with previously described *mum1* and *mum2* mutants (Fig. 1, O and P; Western et al., 2001).

LUH and *MUM1* Are Genetically Identical

Given the similarity in mucilage extrusion defects, we next considered whether *mum1* and *mum2* mutants have other phenotypes in common with *luh*. As *luh* mutants have a notable reduction in root growth (Sitaraman et al., 2008), we compared the length of *luh*, *mum1*, and *mum2* roots with the wild type after 10 d of growth on vertical plates (Fig. 2A). *mum1* and *luh* roots were significantly shorter than wild-type roots (*t* test: *luh*, $P < 0.001$, $n = 28$; *mum1*, $P < 0.004$, $n = 28$; Fig. 2, A and B), whereas *mum2* roots were similar in length to the wild type (*t* test: $P > 0.7$; Fig. 2, A and B).

The striking similarity between the *luh* and *mum1* phenotypes prompted us to consider whether *MUM1* and *LUH* are genetically identical. To test for allelism, *luh* and *mum1* mutants were crossed, and seeds produced by the F1 plants were examined for a mucilage extrusion defect. All 24 F1 plants tested produced seeds that failed to release mucilage, whereas plants derived from a cross between *luh* and *mum2* produced seeds that extrude mucilage normally (data not shown). To confirm that the lesion in *mum1* resides at the *LUH* locus, we amplified and sequenced approximately 4.6 kb of genomic DNA spanning the entire *LUH* coding region from *mum1-1* mutants. This identified a C-to-T change at nucleotide 531 (as measured from the translational start) that is predicted to convert Glu-97 to a stop codon in the sixth exon (Fig. 2C). As this lesion is similar to the strong *luh-1* allele (Fig. 2C; Sitaraman et al., 2008), it is likely that *mum1-1* also conditions a strong loss of function.

To confirm that lesions at the *LUH* locus are responsible for the mucilage extrusion defects, we showed that expressing the *LUH* cDNA sequence from the previously characterized 2.6-kb *LUH* promoter (Stahle et al., 2009) was sufficient to restore mucilage extrusion in seeds derived from 38 of 41 primary *luh* transformants (Fig. 2D). The remainder showed partial or no complementation.

LUH Regulates *MUM2* in the Developing Seed

In addition to having similar mucilage extrusion defects, the MSC of *luh* and *mum2* also have slightly thicker radial cell walls (Fig. 3, A–D). To test whether these phenotypic similarities are a consequence of *LUH* and *MUM2* functioning in the same genetic pathway, we used quantitative reverse transcription (qRT)-PCR to examine the expression of *MUM2* in developing wild-type and *luh* mutant seeds. To ensure that seed coat expression was assayed, we manually separated developing embryos from the seed coat and examined expression in near homogeneous pools of tissue. Detecting expression of the embryo-specific gene *ASYMMETRIC LEAVES1* (Byrne et al., 2000) in two independent pools of embryonic tissue (E_1/E_2) but not seed coat tissue (SC_1/SC_2) confirmed the origin and purity of these samples (Supplemental Fig. S3).

As well as the expected expression in embryos (Stahle et al., 2009), *LUH* expression was also detected in seed coat (testa) samples (Fig. 7D; Supplemental Fig. S3). Absence of PCR products in the *luh* samples indicates that the T-DNA insertion in *luh-4* (Fig. 2C) causes a significant decrease in *LUH* transcript abun-

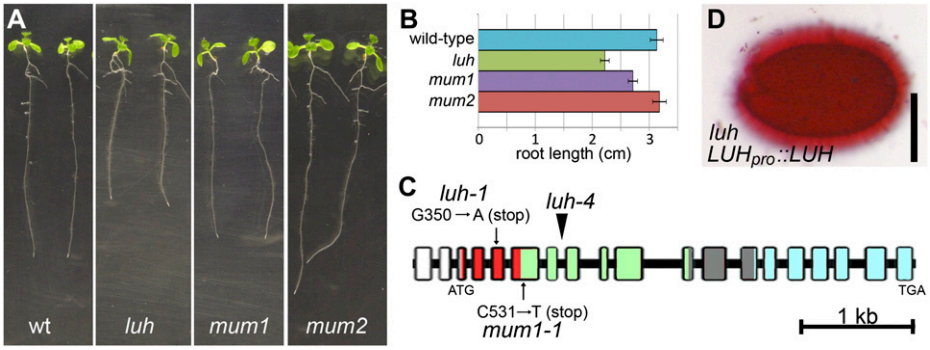

Figure 2. Phenotypic similarity between *luh* and *mum* mutants. A, Ten-day-old plants grown on vertical plates. B, Histogram showing root length after 6 d of growth on vertical plates. Error bars represent SE. C, Structure of *LUH*, with boxes representing exons and lines between the boxes representing introns. Colors indicate the following features: 5′ untranslated region (white), LUFS domain (red), Gln-rich domain (green), variable region (gray), and WD40 domain (blue). The arrowhead indicates the T-DNA insertion allele used in this study, and arrows indicate ethyl methanesulfonate-induced mutations. For the ethyl methanesulfonate alleles, the positions of the altered nucleotides are given relative to the translation initiation site. D, Representative seed from a *luh*;LUH_{pro}::*LUH* plant displaying a wild-type pattern of ruthenium red staining. Bar = 250 μm.

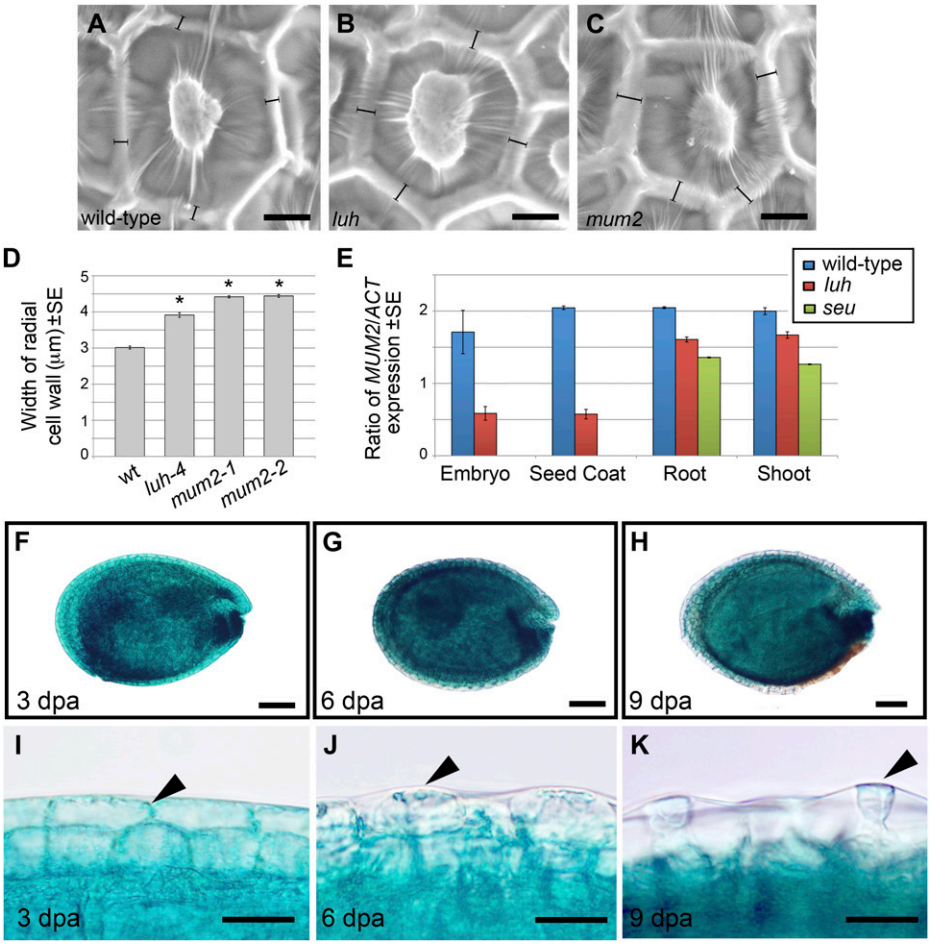

Figure 3. LUH regulates *MUM2* in the developing seed. A to C, Scanning electron micrographs of wild-type (A), *luh-4* (B), and *mum2-1* (C) seeds showing the hexagonal MSC of the testa. Bracketed lines indicate measurements taken of radial wall width. D, Histogram showing the average width of wild-type (wt) and mutant radial cell walls ($n > 50$). Error bars represent SE. Statistical differences between the wild type and mutants were calculated using Student's *t* test, with $P < 0.001$ indicated by asterisks. E, qRT-PCR analysis of *MUM2* expression in embryonic and seed coat tissue collected from 10-dpa wild-type and *luh-4* siliques as well as shoot and root tissue of *luh* and *seu* mutants. F to H, Histochemical localization of LUH_{pro}::*GUS* expression in seeds harvested from siliques at 3 dpa (F), 6 dpa (G), and 9 dpa (H). I to K, Higher magnification of seeds shown in F to H revealing GUS staining (arrowheads) in the epidermis of the testa. Bars = 10 μm in A to C, 100 μm in F to H, and 20 μm in I to K.

dance and thus likely represents an RNA null allele (Fig. 7D; Supplemental Fig. S3). As reported previously, *MUM2* expression was detected in both embryonic and testa tissue (Fig. 3E; Dean et al., 2007; Macquet et al., 2007b). Consistent with LUH regulating *MUM2*, there was an approximately 3-fold reduction of *MUM2* expression in *luh* seed coat and embryonic samples (Fig. 3E). To determine whether *MUM2* expression was affected in other tissues of the plant, we next assayed *luh* shoot and root tissue. While not as dramatic as the reduction seen in seeds, *MUM2* expression was reduced by 16.5% in *luh* shoot tissue and by 21.5% in *luh* root tissue in comparison with the wild type (*t* test: shoot, $P < 0.04$; root, $P < 0.007$; Fig. 3E).

Using previously generated LUH_{pro}::*GUS* plants, we examined *LUH* promoter activity in developing seeds. Consistent with published in situ data, LUH_{pro} activity was detected at all stages of embryo development (data not shown; Stahle et al., 2009). In addition, GUS activity was also apparent throughout the maturing seed coat (Fig. 3, F–H). Higher magnification revealed blue GUS stain in the periphery of MSC at 3 dpa (Fig. 3I), whereas by 6 dpa, it had shifted centrally (Fig. 3J). At lower levels, stain was also apparent in the cytoplasmic column of MSC at 9 dpa (Fig. 3K).

Previous work has shown that LUH physically interacts with the coregulator SEUSS (SEU) in yeast (Sitaraman et al., 2008; Stahle et al., 2009), suggesting that such interactions may be important for LUH function. To determine whether SEU also functions upstream of *MUM2*, we used qRT-PCR to examine *MUM2* expression in shoot and root tissue derived from *seu* mutants. This revealed a 36.8% reduction in shoot tissue and a 33.6% decrease in root tissue (*t* test: shoot, $P < 0.005$; root, $P < 0.0005$; Fig. 3E), which is consistent with SEU and LUH being part of the same regulatory complex.

In summary, our analysis shows that LUH/MUM1 is a major regulator of *MUM2* expression in developing seeds and, to a lesser extent, in other tissues of the plant.

Altered HG Esterification Is Detected in *luh* and *mum2* MSC

Previous characterization of *mum1* and *mum2* mucilage has identified several structural modifications that may influence the degree of pectin swelling following hydration (Western et al., 2001; Dean et al., 2007; Macquet et al., 2007b). The first is an apparent 6%

to 8% increase in the level of pectin methyl esterification detected in ammonium oxalate-extracted mucilage from both *mum* mutant lines (Western et al., 2001). However, owing to the different extractability of *mum* and wild-type mucilage, direct comparisons between these samples is potentially misleading. Thus, to avoid issues associated with extraction, we used immunoelectron microscopy to examine the extent of methyl esterification present in wild-type and *luh* mutant MSC in seeds harvested from 12-dpa siliques. It is expected that, at this stage of development, mucilage modification has ceased, as the epidermal cells are fully differentiated and beginning to desiccate. The methyl esterification status of HG was selected for analysis because previous studies have found that the main component of mucilage, RG-I, is not substantially methyl esterified (Penfield et al., 2001; Macquet et al., 2007a). Monoclonal antibodies JIM5 and JIM7 were used for this analysis, as they recognize sparsely and heavily methyl esterified HG, respectively (Knox et al., 1990; Willats et al., 2000, 2001). A secondary antibody conjugated to gold (18 nm) was then used to visualize binding to HG epitopes.

JIM5 labeling of wild-type and *luh* mutant cells detected clumps of sparsely methyl esterified HG within the secreted mucilage present in the apoplastic space interior to the cell wall of seed coat epidermal cells (Fig. 4, A and B). This contrasts with a much more even distribution of epitopes within the primary cell wall (Fig. 4, C and D). Labeling with JIM7 revealed few heavily methyl esterified HG epitopes in either the apoplastic space or the primary cell wall of wild-type cells (Fig. 4, F and H). Interestingly, the frequency of JIM7 labeling was noticeably elevated in the *luh* mutant (Fig. 4, G and I), consistent with the increased methyl esterification previously reported for this line (Western et al., 2001).

Increased RG-I Substitution Is Detected in *luh* Mucilage

In addition to altered pectin methyl esterification, increased RG-I substitution is also a feature of *mum2* mucilage (Dean et al., 2007; Macquet et al., 2007b). Given that *MUM2* expression is reduced in *luh* mutants, we used linkage (by methylation) analysis to characterize the sugar linkages present in mucilage extracted from *luh* seeds using hot acid and then strong alkali (see "Materials and Methods"). Based on ruthenium red staining of seeds following these treatments (Supplemental Fig. S4), the acid-soluble fraction contains loosely attached pectins from the outer water-soluble layer and possibly those from the inner layer. The remainder of the strongly associated pectins and cross-linking glycans (hemicellulose/cellulose) from the inner mucilage layer were largely solubilized following extended alkali treatment. These fractions were then subjected to carboxyl reduction and methylation before partially methylated alditol acetates were quantified by gas chromatography-mass spectrometry (GC-MS). Data are presented as mol % (Table I).

As reported previously, the predominant linkages present in mucilage from wild-type seeds are 2-linked Rha (2-Rha*p*) and 4-linked GalA (4-GalA*p*) with a small quantity of 2,4-linked Rha (2,4-Rha*p*; Table I; Penfield et al., 2001; Western et al., 2004). Interestingly, the degree of RG-I substitution differed between fractions, with the substituted (2,4-Rha):unsubstituted (2-Rha) Rha ratio being approximately 1:42 in the acid-soluble fraction and approximately 1:14 in the alkali-soluble fraction (Table II). Modest increases in sugars associated with arabinan and (arabino)-3,6-galactan side chains were also observed in the alkali-soluble fraction, including terminal Ara (*t*-Ara*f*), 5-Ara*f*, 2,5-Ara*f*, 3-Gal*p*, 6-Gal*p*, and 3,6-Gal*p* residues. Similarly, increases in terminal Gal (*t*-Gal*p*) and 4-Gal*p* residues

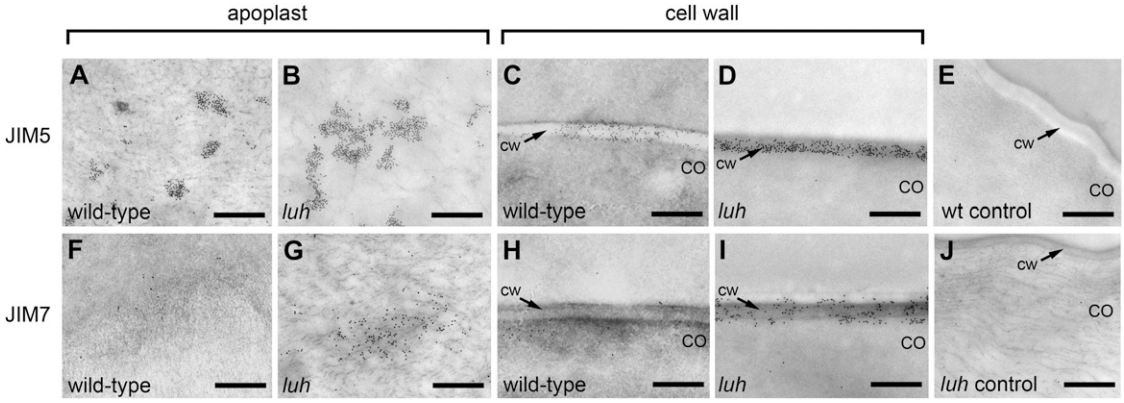

Figure 4. Distribution of methyl-esterified HG epitopes in epidermal cells of the testa. A to D and F to I, Transmission electron microscopy of sections through 12-dpa seeds labeled with JIM5 (A–D) and JIM7 (F–I) antibodies. HG epitopes bound by primary antibodies were visualized with a secondary antibody conjugated to gold (black dots). Micrographs show labeling of HG epitopes in the apoplasts of wild-type (A and F) and *luh-4* (B and G) epidermal cells of the seed coat and labeling of HG epitopes in the primary cell walls (CW) of wild-type (C and H) and *luh-4* (D and I) epidermal cells of the seed coat. CO, Columella. E and J, Micrographs showing background labeling with secondary antibody in the absence of primary antibody. Bars = 0.5 μm.

Table I. *Sugar linkage composition of extracted mucilage from wild-type, luh, and mum2 seeds*

Soluble polysaccharides from intact seeds were extracted sequentially with acid (HCl soluble) and alkali (NaOH soluble). Samples were neutralized, and following methylation, the partially methylated alditol acetates were quantified by GC-MS. Results are given as mol % ± SE calculated from two independent experiments (wild type and *luh*). ND, Not detected; tr, trace (less than 0.5 mol %).

Sugar and Linkage	HCl Soluble			NaOH Soluble		
	Wild Type	*luh*	*mum2*	Wild Type	*luh*	*mum2*
Rha						
t-Rha*p*	0.9 ± 0.5	tr	0.5	1.0 ± 0.0	0.9 ± 0.1	tr
2-Rha*p*	44.1 ± 4.6	28.3 ± 1.5	30.9	28.5 ± 3.9	22.8 ± 1.2	23.0
2,4-Rha*p*	1.0 ± 0.5	7.0 ± 3.2	5.7	2.4 ± 0.2	9.2 ± 0.7	5.8
Total	46	35.3	37.1	31.9	32.9	28.8
Ara						
t-Ara*f*	2.4 ± 0.0	5.0 ± 2.0	3.0	5.9 ± 2.1	4.0 ± 1.9	2.0
2-Ara*f*	0.5 ± 0.2	0.8 ± 0.1	0.6	2.9 ± 2.5	2.2 ± 2.5	2.1
3-Ara*f*	0.5 ± 0.1	0.6 ± 0.1	0.5	1.7 ± 0.8	1.0 ± 0.9	1.1
5-Ara*f*	0.8 ± 0.2	2.0 ± 1.8	1.4	2.0 ± 0.8	1.4 ± 1.4	1.0
2,5-Ara*f*	0.5 ± 0.1	0.6 ± 0.1	0.8	1.1 ± 1.5	0.6 ± 0.9	ND
3,5-Ara*f*	tr	tr	ND	tr	tr	ND
Total	4.7	9	6.3	13.6	9.2	6.2
Xyl						
t-Xyl*p*	tr	0.7 ± 0.6	0.5	3.1 ± 1.4	2.5 ± 1.7	0.5
4-Xyl*p*	tr	1.6 ± 2.2	1.0	5.3 ± 4.2	49.2.9	5.4
Total	0	2.3	1.5	8.4	7.4	5.9
Man						
4-Man*p*	0.5 ± 0.7	1.7 ± 2.4	1.2	1.8 ± 2.5	1.5 ± 2.1	2.1
Gal						
t-Gal*p*	0.8 ± 0.3	8.1 ± 0.7	8.4	1.7 ± 0.3	8.9 ± 0.1	8.0
3-Gal*p*	tr	1.0 ± 0.7	0.8	1.3 ± 0.0	1.0 ± 0.2	4.0
4-Gal*p*	0.6 ± 0.3	0.9 ± 0.8	tr	1.1 ± 1.1	1.1 ± 1.1	ND
6-Gal*p*	tr	tr	ND	0.5 ± 0.8	tr	ND
3,6-Gal*p*	tr	0.6 ± 0.9	ND	0.5 ± 0.7	0.5 ± 0.7	ND
Total	1.4	10.6	9.2	5.1	11.5	12
Glc						
t-Glc*p*	tr	tr	tr	1.6 ± 1.8	1.2 ± 1.1	2.1
2-Glc*p*	tr	tr	ND	tr	1.2 ± 0.7	1.5
4-Glc*p*	0.9 ± 0.3	1.9 ± 1.5	7.9	4.5 ± 1.4	2.5 ± 0.7	7.9
3,4-Glc*p*	tr	tr	ND	0.7 ± 1.1	0.7 ± 1.0	ND
Total	0.9	1.9	7.9	6.8	5.6	11.5
GalUA						
t-GalA*p*	1.0 ± 0.3	0.9 ± 0.7	1.5	1.0 ± 0.1	1.2 ± 0.4	tr
4-GalA*p*	42.0 ± 1.3	35.1 ± 2.4	33.9	28.6 ± 0.7	30.1 ± 0.1	32.5
Total	43	36	35.4	29.6	31.3	32.5
GlcA						
t-GlcA*p*	tr	0.7 ± 0.5	0.7	1.1 ± 1.6	0.5 ± 0.1	tr

were also detected, suggesting that individual Gal residues and (arabino)-4-galactan side chains are attached to the RG-I backbone in alkali-extracted mucilage (Table I).

Analysis of mucilage extracted from *luh* seeds revealed near wild-type levels of 4-GalA*p* in the alkali-soluble fraction but reduced levels in the acid-soluble fraction (Table I). In comparison with wild-type mucilage, levels of the substituted 2,4-Rha*p* residues were significantly elevated and 2-Rha*p* residues were reduced in both the acid- and alkali-soluble mucilage fractions obtained from *luh* mutants (Table I; Fig. 5, A and B). As a result of these changes, the ratio of substituted (2,4-Rha) to unsubstituted (2-Rha) Rha in the acid- and alkali-soluble fractions of *luh* mutants was approximately 1:4 and approximately 1:3, respectively (Table II). Correlated with changes in *luh* RG-I structure was a substantial increase in *t*-Gal*p* residues, with an approximately 10-fold increase observed in the acid-soluble fraction and an approximately 5-fold increase in the alkali-soluble fraction (Table I; Fig. 5, C and D). Moderate increases in *t*-Ara*f* and 5-Ara*f* residues were also detected in the acid-soluble fraction but not in the alkali-soluble fraction (Table I; Fig. 5, C and D). While changes to RG-I structure are the most obvious defect in *luh* mutant mucilage, small changes in the distribution of xylans, galacto(gluco)mannans, and residues belonging to arabino-3,6-galactan side chains of either RG-I or arabinogalactan proteins were also observed (Table II).

To confirm that the *luh* mucilage structure was similar to that of *mum2* mutants, we determined the

Table II. *Calculated polysaccharide composition (mol %) of extracted mucilage from wild-type, luh, and mum2 seeds*

Polysaccharide	HCl Soluble			NaOH Soluble		
	Wild Type	*luh*	*mum2*	Wild Type	*luh*	*mum2*
Arabinan	2.7	4.6	4.0	8.8	5.9	4.3
Type I arabinogalactan	0.6	0.9	0.0	1.1	1.1	0.0
Type II arabinogalactan	2.3	2.8	4.0	2.0	0.8	0.0
Arabinoxylan	0	1.6	1.0	5.3	4.9	5.4
Galacto(gluco)mannan	0.5	1.7	1.2	1.8	1.5	2.1
HG	0	0	0	0	0.4	3.8
RG-I (substituted:unsubstituted ratio)	91.4 (1:42.3)	77.6 (1:4.0)	78.8 (1:5.5)	63.1 (1:14.2)	66.2 (1:3.3)	63.2 (1:4.0)
Other	2.5	10.8	11.0	18.0	19.3	21.2

linkage composition of *mum2* mucilage. The changes detected in RG-I structure closely paralleled those seen in *luh* mutants and were also similar to the published *mum2* mucilage structure (Tables I and II; Fig. 5; Dean et al., 2007; Macquet et al., 2007b). Structural similarity between *luh* and *mum2* mutant mucilage is consistent with a loss of MUM2 activity in *luh* mutant seeds.

Heterologous *MUM2* Expression Restores Mucilage Release from *luh* Seeds

The striking similarity between *luh* and *mum2* RG-I structure together with low-level *MUM2* expression in *luh* mutant seeds strongly suggested that LUH regulates *MUM2* activity in the developing seed coat. To further test this hypothesis, we used a transgenic approach to restore *MUM2* expression in developing *luh* seeds. Because *LUH* and *MUM2* have similar expression profiles (Fig. 3, I–K; Dean et al., 2007; Macquet et al., 2007b), we reasoned that the *LUH* promoter might be suitable to drive *MUM2* expression in the developing seed coat. Therefore, we introduced a LUH_{pro}::*MUM2* construct into *mum2* mutants and used ruthenium red staining to assess mucilage release from seeds produced by T1 transgenic plants. Based on the staining pattern, we distinguished four categories of transgenic plant. Class I plants produced seeds with wild-type levels of mucilage release that stained well with ruthenium red (n = 27; Fig. 6A). Class II plants produced seeds that released wild-type levels of mucilage but, unlike seeds from the first class, stained poorly with ruthenium red (n = 14). The next two classes of plants produced seeds that either released small quantities of mucilage (class III; n = 21) or completely failed to release mucilage (class IV; n = 28). Finding full mucilage release in seeds obtained from approximately one-third of *mum2* transformants confirmed that the *LUH* promoter was sufficiently active

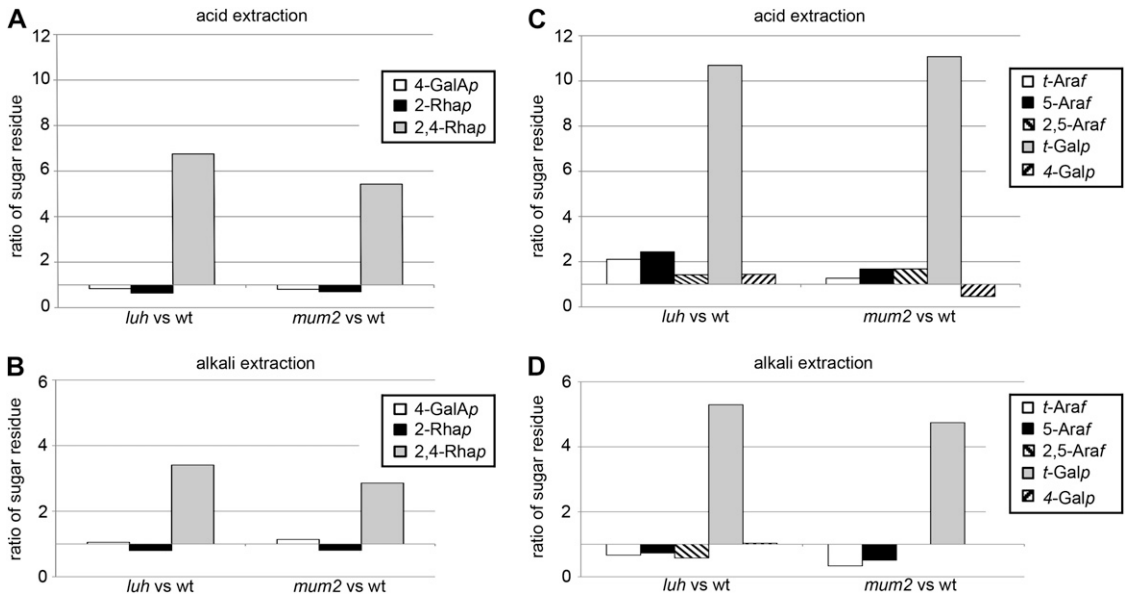

Figure 5. Changes in the proportion of sugar linkages present in *luh* and *mum2* mutant mucilage in comparison with the wild-type (wt). Histograms show the change in proportion of monosaccharide residues associated with the RG-I backbone (A and B) and arabinan/(arabino)galactan side chains (C and D) present in mucilage extracted with acid (A and C) and alkali (B and D) relative to the wild type as determined by GC-MS (the complete data set is shown in Table I). Inset legends indicate each monosaccharide and its linkage.

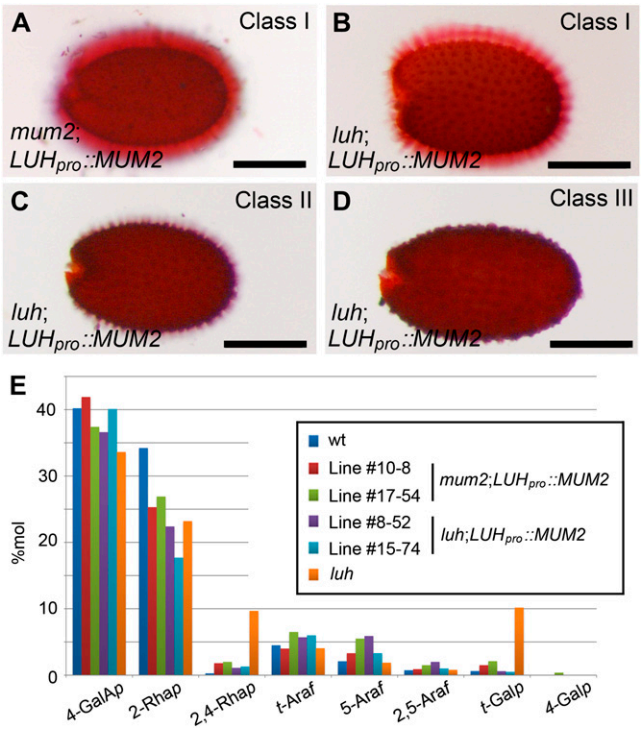

Figure 6. Heterologous *MUM2* expression in mutant lines. A, Seed obtained from a class I primary *mum2*;LUH_{pro}::*MUM2* transformant showing restored mucilage extrusion following ruthenium red staining. B to D, Seeds obtained from class I (B), class II (C), and class III (D) primary *luh*;LUH_{pro}::*MUM2* transformants. Bars = 250 μm. E, Histogram showing mol % of sugar linkages associated with the RG-I backbone and side chains present in the alkali-soluble fraction of mucilage extracted from wild-type (wt) and transgenic mutant lines. The complete data set is presented in Supplemental Table S1.

to compensate for the loss of endogenous *MUM2* activity in *mum2* mutants. Having established the utility of the *LUH* promoter, we next introduced the LUH_{pro}::*MUM2* construct into *luh* mutants. In this case, approximately one-quarter of primary transformants displayed full complementation (class I; n = 33; Fig. 6B), while the remaining transformants produced seeds with a class II phenotype (n = 47; Fig. 6C), a class III phenotype (n = 31; Fig. 6D), or a class IV phenotype (n = 10; data not shown).

To confirm that heterologous *MUM2* expression in developing *mum2* and *luh* seeds produces a wild-type mucilage structure, methylation analysis was conducted on seed mucilage extracted from two independently derived *mum2*;LUH_{pro}::*MUM2* class I lines and two independently derived *luh*;LUH_{pro}::*MUM2* class I lines (Fig. 6E; Supplemental Table S1). Due to the large number of samples, we confined our analyses to alkali-soluble mucilage. Based on the relative abundance of residues associated with the RG-I backbone and its side chains, mucilage obtained from transgenic seeds had a structural profile similar to the wild type (Fig. 6E). For instance, the increased proportions of branched Rha residues (2,4-Rha) and *t*-Gal*p* residues found in *luh* and *mum2* mucilage (Fig. 5; Table I) were not observed in mucilage from transgenic lines (Fig. 6E; Supplemental Table S1). Subsequent qRT-PCR analysis confirmed that *MUM2* expression was close to wild-type levels in 10-dpa seed tissue obtained from two independent class I *luh*;LUH_{pro}::*MUM2* lines (Table III). This confirms that elevating *MUM2* expression in *luh* mutants restores RG-I substitution to wild-type levels and reestablishes mucilage extrusion.

LUG Functions Redundantly with LUH to Promote Mucilage Extrusion from the Testa

Previous work has shown that *LUG* and *LUH* regulate overlapping processes in vegetative and floral development (Sitaraman et al., 2008; Stahle et al., 2009). To determine whether this is also the case in the seed coat epidermis, we characterized *luh* mutant seeds lacking *LUG* activity. Due to *lug;luh* double mutants being embryo lethal (Sitaraman et al., 2008), we focused on seeds derived from plants homozygous for *luh* and heterozygous for *lug* (*luh;lug*/+). Although *lug* segregation occurs embryonically, all seeds derived from this line have a *luh;lug*/+ seed coat genotype due to this tissue being maternal in origin.

In contrast to *luh* mutants, no mucilage was released from seeds arising from *luh;lug*/+ plants following EDTA treatment (compare Fig. 1N and Fig. 7A). The presence of mucilage in the *luh;lug*/+ seed coat was subsequently confirmed by sectioning wax-embedded seeds and staining with ruthenium red (Fig. 7B). As mucilage is released from *lug* mutant seeds following hydration (Fig. 7C), the role of LUG in the seed coat is only apparent when LUH activity is compromised. Consistent with *LUG* having a role in the developing seed, qRT-PCR assays detected *LUG* expression in both embryonic and seed coat tissue (Fig. 7D). However, when compared with *LUH*, *LUG* expression was substantially (approximately 3-fold) lower in the seed coat tissue.

Given that the enhanced extrusion defect of the *luh;lug*/+ seeds was not associated with an obvious reduction in mucilage accumulation within the MSC (Supplemental Fig. S5), we next addressed whether this phenotype was correlated with a further decrease in *MUM2* expression. qRT-PCR analysis, however, failed to detected a significant expression difference

Table III. *qRT-PCR analysis of MUM2 expression in transgenic lines*

Line	Ratio of *MUM2* to *ACT7* Expression	
	Seed Coat	Embryo
Wild type	1.89	1.83
luh;LUH_{pro}::*MUM2* #8-35	1.51	1.55
luh;LUH_{pro}::*MUM2* #15-74	1.48	1.40
luh;LUH_{pro}::*LUH* #4-1	1.34	1.53
luh;LUH_{pro}::*LUH* #5-2	1.34	1.40
luh;LUH_{pro}::*LUG* #2	1.34	1.27
luh;LUH_{pro}::*LUG* #12	1.41	1.49

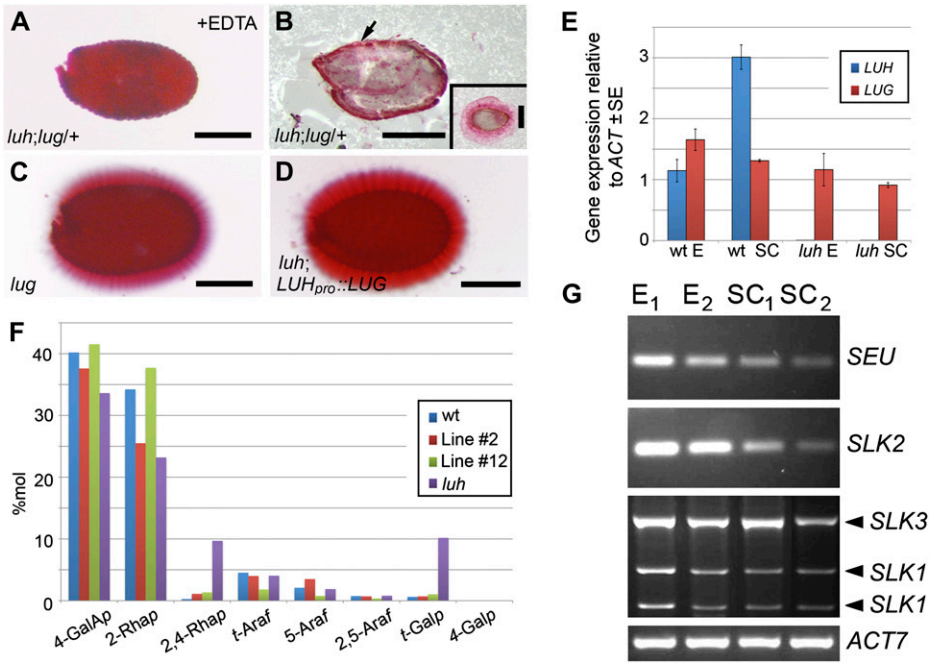

Figure 7. Redundancy between *LUH* and *LUG*. A, Ruthenium red-stained seed obtained from a *luh;lug*/+ plant following a 2-h EDTA treatment. B, Ruthenium red-stained section of a wax-embedded seed obtained from a *luh;lug*/+ plant. Mucilage staining is indicated with the arrow. The inset shows a wild-type seed section stained with ruthenium red. C and D, Ruthenium red-stained seeds from *lug* mutant (C) and *luh;LUH*$_{pro}$::*LUG* transgenic (D) plants displaying wild-type levels of mucilage release. Bars = 250 μm. E, qRT-PCR analysis of *LUH* and *LUG* expression in embryo (E) and seed coat (SC) samples obtained from wild-type (wt) and *luh* 10-dpa siliques. F, Histogram showing mol % of sugar linkages associated with the RG-I backbone and side chains present in the alkali-soluble fraction of mucilage extracted from wild-type and transgenic *luh;LUH*$_{pro}$::*LUG* lines. The complete data set is presented in Supplemental Table S1. G, RT-PCR analysis of *SEU*, *SLK1-3*, and *ACT7* expression in embryo (E_1 and E_2) and seed coat (SC_1 and SC_2) samples obtained from wild-type 10-dpa siliques.

between *luh* and *luh;lug*/+ seed coats (data not shown). As an alternative strategy to determine whether LUG has a role in seed coat development, we placed the *LUG* coding region under the control of the *LUH* promoter and introduced the construct into *luh* mutants. Of the 42 primary transformants, 39 plants produced seeds with a wild-type pattern of mucilage extrusion (Fig. 7E). To confirm that the *luh;LUH*$_{pro}$::*LUG* transgenic plants produce mucilage with a wild-type structure, we performed linkage analysis on mucilage extracted from two independent *luh;LUH*$_{pro}$::*LUG* transgenic lines (Supplemental Table S1). Consistent with LUG and LUH being functionally interchangeable, levels of sugar linkages normally associated with a wild-type RG-I backbone and side chains were present in the transgenic mucilage (Fig. 7F; Supplemental Table S1). Furthermore, qRT-PCR analysis detected similar levels of *MUM2* expression in both *luh;LUH*$_{pro}$::*LUH* and class I *luh;LUH*$_{pro}$::*LUG* seed coat tissue (Table III). While these data confirm the functional equivalence of LUG and LUH, differences in expression level presumably account for their unequal roles within the seed coat.

Recruitment of the corepressor LUG, and presumably LUH, to regulatory sequences of target genes is dependent on physical interactions with the coregulator SEU. Therefore, we examined whether *SEU* and the closely related *SEU-LIKE* (*SLK1–SLK3*) genes (Stahle et al., 2009; Bao et al., 2010) are expressed in embryonic and seed coat tissue. Consistent with redundancy between these coregulators, RT-PCR analysis detected expression of all four genes in these tissues (Fig. 7G).

DISCUSSION

This study has established that mutations in *LUH*, a gene closely related to the transcriptional corepressor *LUG* (Liu and Karmarkar, 2008), affect mucilage release from the seed coat following contact with water. Mutants lacking mucilage extrusion can be grouped according to whether they either disrupt the differentiation of the seed coat or specifically interfere with mucilage biosynthesis and/or structure (for review, see Western, 2006). Based on our cytological analysis, *luh* mutants belong to this second group, as seed coat differentiation and mucilage secretion into the apoplast are largely unaltered.

Relationship between *LUH* and *MUM* Genes

Phenotypic similarity between *luh* and the well-characterized mucilage extrusion-defective mutants

mum1 and *mum2* (Western et al., 2001) suggested that these genes might function in the same pathway. Through a series of genetic crosses, we established that *luh* and *mum1* mutations were allelic and subsequently identified a lesion at the *LUH* locus in *mum1-1* mutants. Given that *LUH* encodes a transcriptional regulator (see below) and *MUM2* encodes a β-galactosidase, we addressed whether *LUH* might regulate *MUM2*. Our analyses provide two lines of evidence in support of such regulatory arrangement. First, we found significant overlap in *LUH* promoter activity, as assessed by GUS assays, and *MUM2* expression in both the developing seed coat and other tissues of the plant (Macquet et al., 2007b; Stahle et al., 2009; this study). Next, we showed by qRT-PCR that there is an approximately 3- to 4-fold reduction of *MUM2* expression in both seed coat and embryo tissue of *luh* mutants as well as smaller changes in the shoots and roots of these mutants. Based on these observations, we propose that LUH is a global regulator of *MUM2* and that loss of *MUM2* activity from the *luh* seed coat causes the mucilage extrusion defect. Consistent with this hypothesis, restoring *MUM2* expression in *luh* seeds results in normal mucilage release when exposed to water. Whether the root growth defect observed in *luh* mutants is also a consequence of reduced *MUM2* activity remains to be seen, although lack of root growth defects in *mum2* mutants makes this scenario seem unlikely.

Altered RG-I Structure in *luh* Mutants

Loss of MUM2 (β-galactosidase) activity in *luh* mutant seeds prompted us to examine the structure of *luh* mucilage. Analysis of mucilage extracted from *luh* mutants revealed significantly more side chain substitution of RG-I in both acid- and alkali-soluble fractions when compared with the wild type. The majority of side chain residues were terminal Gal residues, although residues associated with linear arabinan side chains were apparent in the acid-soluble fraction. Finding an almost identical RG-I substitution profile associated with *mum2*-extracted mucilage (Dean et al., 2007; Macquet et al., 2007b; this study) provides additional evidence for the structural changes in *luh* mucilage arising from a loss of *MUM2* activity. This conclusion is further corroborated by a return to a wild-type ratio of substituted (2,4-Rha) to unsubstituted (2-Rha) Rha residues in mucilage of transgenic *luh* seeds in which *MUM2* expression is restored.

Although weakening the cell wall of *luh* mutant seeds results in mucilage release, it does not swell to the same extent as wild-type mucilage. Finding similar defects in *mum2* mucilage (Western et al., 2001; Dean et al., 2007; Macquet et al., 2007b) suggests that increased RG-I substitution affects the hydration properties of mucilage. Consistent with this observation, increased RG-I substitution with arabinan side chains is correlated with a slow and patchy release of mucilage from *bxl1* mutant seeds (Arsovski et al., 2009). In contrast, removing galactan side chains from avocado (*Persea americana*) pectin using a β-D-galactosidase increased solubility by reducing the molecular size and aggregation potential of pectin molecules (De Veau et al., 1993). In this respect, it is interesting that the biophysical properties of the inner and outer mucilage layers of Arabidopsis seeds differ. Mucilage present in the outer layer has a smaller molecular mass and increased solubility compared with the inner layer, which forms an insoluble dense gel of high molecular mass (Macquet et al., 2007a). Given that the extent of RG-I substitution varies between the layers, it is likely that the biophysical properties of each layer are largely determined by their RG-I composition. Increased RG-I substitution observed in both *luh* and *mum2* mucilage, therefore, is expected to increase the molecular mass and aggregation potential of pectin and substantially reduce mucilage solubility. As a consequence, mutant mucilage will not swell to the same extent as the wild type following hydration and, hence, will exert less physical force on the outer cell wall of the MSC, either severely restricting or preventing the rupturing of these cells.

Although little is known about how RG-I substitution influences the hydration properties of mucilage, it is clear that highly substituted RG-I has a larger molecular mass than unsubstituted RG-I (Macquet et al., 2007a). Based on the observation that the degree of RG-I substitution influences the activity of RG-I backbone-degrading enzymes such as RG hydrolase and RG lyase (Azadi et al., 1995; Mutter et al., 1998), we propose that RG-I backbone-degrading enzymes are also active in the apoplast of mucilage-secreting cells. Accordingly, substituted RG-I present in the inner layer will not be processed by the RG-I backbone-degrading enzymes to the same extent as unsubstitutedRG-I in the outer layer and thus will have a larger molecular mass. Although there are several classes of RG-I backbone-degrading enzymes, only RG lyases have been unambiguously identified in planta (Naran et al., 2007). Based on sequence alignments with bacterial and fungal lyase sequences, it is predicted that a small RG lyase family is present in the Arabidopsis genome (Coutinho and Henrissat, 1999). Thus, it is conceivable that these enzymes might be active in the developing seeds where they target RG-I for degradation. Greater substitution of the RG-I backbone in *luh* and *mum2* mutant mucilage will likely block access of the RG-I backbone-degrading enzymes to the RG-I backbone, presumably as a result of steric hindrance. Failure to process the RG-I will result in the mutant mucilage having a larger molecular mass, which in turn is likely to alter its hydration properties. An important test of this model will be to determine whether the loss of RG-I backbone-degrading activity in the mucilage-secreting cells of the testa is associated with a mucilage extrusion defect. Presumably, this defect would arise from unsubstituted RG-I no longer being processed into smaller polymers.

Increased Methyl Esterification of HGs in *luh* Mucilage

In addition to alterations in RG-I substitution, changes in the pattern of HG methyl esterification were also detected within the apoplastic space and primary cell walls of *luh* seed coat epidermal cells using immunoelectron microscopy analysis. Assuming that the process of HG modification in the apoplast of mucilage-secreting cells is similar to that of cell walls (Schols and Voragen, 1996), it is likely that HG is secreted in a highly methyl esterified form and subsequently deesterified by a family of pectin methylesterases (PMEs) in the apoplast. The increased HG methyl esterification observed in *luh* mucilage, therefore, could reflect a role for *LUH* in promoting PME expression during seed coat maturation. However, as increased methyl esterification has been observed in extractable *mum2* mucilage (Western et al., 2001), it is possible that PME activity is altered in response to RG-I modification. According to this possibility, LUH would not be a direct regulator of PME activity but would function indirectly via RG-I modification. Future work will need to distinguish between these possibilities.

On the basis of immunofluorescence studies, two distinct populations of HG are distinguishable in the inner mucilage layer. Heavily methyl esterified HG localizes in the periphery of the inner layer, whereas sparsely methyl esterified HG is enriched in a region directly adjacent to the epidermal cell wall. Thus, based on these observations, it is likely that the dense gel-like matrix formed by the inner mucilage layer is due in part to calcium-based cross-linking between sparsely esterified HG polymers (Willats et al., 2001; Macquet et al., 2007a). Consistent with reduced HG methyl esterification affecting the hydration properties of mucilage, increased PME activity in developing seeds of *atsbt1.7* mutants results in a mucilage extrusion defect (Rautengarten et al., 2008). Conversely, increased methyl esterification of HG present in the inner layer of *mum5* mutants (M. Facetter and C. Somerville, personal communication, cited in Western, 2006) did not adversely affect mucilage release from the testa but instead reduced the gelling properties of the inner layer. Based on these observations, it is unlikely that the increased HG methyl esterification observed in *luh* mucilage can explain the extrusion defects observed in this line.

Redundancy between LUH and LUG

Of the 13 Gro/Tup1 corepressors in Arabidopsis, LUG and LUH share the greatest similarity, with over 80% sequence identity in the N-terminal LUFS domain as well as extensive identity in the C-terminal WD repeats and adjacent sequences (Liu and Karmarkar, 2008). Thus, it is not surprising to find that these genes function redundantly in a number of processes, including early embryonic development and postembryonic leaf, shoot, and flower development (Sitaraman et al., 2008; Stahle et al., 2009). In postembryonic development, redundancy between *LUG* and *LUH* was inferred from the enhancement of *lug* phenotypes when *luh*/+ was present in the background, as *lug;luh* double mutants are embryo lethal. While the mucilage extrusion defects of seeds derived from *lug* mutants heterozygous for *luh*/+ could not be assessed due to infertility of *lug;luh*/+ flowers, seeds derived from *luh* mutants heterozygous for *lug* displayed an enhanced mucilage extrusion defect following treatment with EDTA. Furthermore, transgenic experiments clearly indicate that LUG and LUH are functionally equivalent, although mutations in these genes do not condition identical phenotypes. For instance, *lug* mutants release mucilage following contact with water, whereas *luh* mutants do not. A possible explanation for this difference emerged from our qRT-PCR analysis, which detected substantially higher levels of *LUH* expression in the developing seed coat, in comparison with *LUG*. This observation supports the view that the cis-regulatory elements of these genes have diverged so that *LUG* is no longer expressed at high levels within the seed coat. Analysis of the publicly available microarray data has also identified differences in the

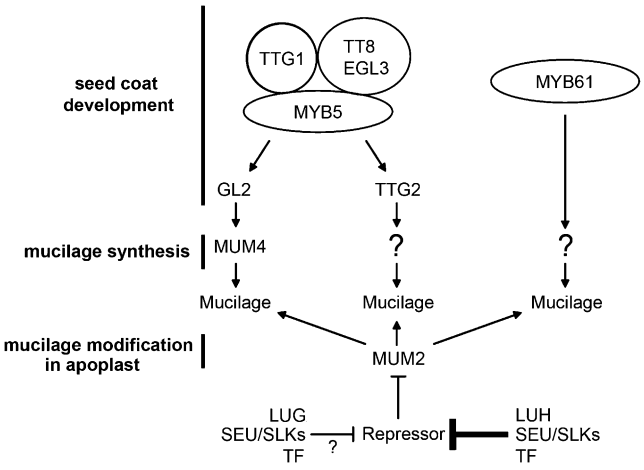

Figure 8. A model for the role of LUH in regulating mucilage modification in seed coat epidermal cells. Epidermal seed coat differentiation is controlled by a multimeric complex that includes MYB5, bHLH proteins (TT8/EGL3), and a WD40 repeat protein, TTG1 (Li et al., 2009). This complex is thought to positively regulate *GL2*. GL2 in turn activates *MUM4*, an NDP-L-Rha synthase required for the synthesis of RG-I (Western et al., 2004). Although MYB61 also regulates seed coat differentiation and mucilage synthesis, it is thought to function via a separate pathway (Western et al., 2004). *MUM2* encodes a secreted glycosidase that removes Gal residues from the RG-I side chains in the apoplast (Dean et al., 2007; Macquet et al., 2007b). We propose that LUH may promote *MUM2* expression indirectly through the repression of a negative regulator (repressor). LUH is likely to perform this function by forming a regulatory complex with either SEU or SLK proteins and an as yet unidentified transcription factor (TF). According to this model, reduced LUH activity would lead to increased expression of the *MUM2* repressor, and as a consequence, *MUM2* expression would be reduced. While not unambiguously demonstrated, it is likely that LUG is also capable of regulating *MUM2* activity.

transcriptional responses of *LUG* and *LUH* to abiotic and biotic stress (Sitaraman et al., 2008), which also supports the view that the regulatory responses of these genes have diverged. While our data point to LUG and LUH being functionally interchangeable in the developing seed coat, the same is apparently not true in the developing flower, where constitutive expression of *LUH* fails to restore the floral patterning defects of *lug* mutants (Sitaraman et al., 2008). Why LUG and LUH should have identical functions in one tissue type but not another is unclear at present but could conceivably arise from a differing distribution of cofactors that are required for LUG and LUH function. Candidate cofactors are SEU and the SLK proteins, which display redundant functions in various plant tissues (Stahle et al., 2009; Bao et al., 2010). In this regard, it is interesting that while SEU clearly plays a role in *MUM2* regulation within shoot and root tissue, *seu* mutants do not condition a mucilage extrusion defect. However, given that all three SLK genes are expressed in the seed coat (Fig. 7C), it is likely that there is extensive redundancy between these genes, as noted in previous studies (Stahle et al., 2009; Bao et al., 2010).

Model for LUH Function in the Seed Coat

On the basis of in vivo assays, LUG is found to act as a potent transcriptional repressor when bound to plant or yeast promoters (Sridhar et al., 2004). Given that the domains involved in repression are shared with LUH (Sridhar et al., 2004; Sitaraman et al., 2008), it is probable that LUH also functions as a negative regulator. This view is supported by genetic evidence showing that *luh*/+ enhances *AGAMOUS* misexpression in the outer whorl organs of *lug* mutants (M. Walker, M. Tehseen, M.S. Doblin, F.A. Pettolino, S.M. Wilson, A. Bacic, and J.F. Golz, unpublished data) and *KNOX* misexpression in *lug* mutant leaves (Stahle et al., 2009). However, in the absence of a direct biochemical test, attributing repressor activity to LUH remains speculative.

Nonetheless, finding that LUG restores the mucilage defects of *luh* mutants when expressed under the control of the *LUH* promoter raises the possibility that transcriptional repression is involved in *MUM2* regulation. Taken together with the observed reduction of *MUM2* expression in *luh* mutants, we propose that LUH regulates *MUM2* indirectly. In this model, a LUH-containing complex, and to a lesser extent a LUG-containing complex, directly regulates a *MUM2* repressor (Fig. 8). Loss of LUH activity, therefore, is expected to result in increased activity of the *MUM2* repressor and reduced expression of *MUM2*. Testing this model will require the identification of the *MUM2* repressor, which may be achieved by either defining the targets of the LUH regulatory complex within the developing testa or through the identification of the transcription factors bound by the LUH regulatory complex.

In summary, this study, to our knowledge, is the first to identify a regulatory pathway involved in pectin modification. Although this work has focused on seed mucilage, it is possible given the broad expression pattern of LUH, LUG, SEU, and SLKs (Stahle et al., 2009) that this regulatory complex also controls cell wall pectin structure in other plant tissues. If the role of LUG and LUH as global regulators of pectin-modifying enzymes is confirmed, it will raise the intriguing possibility that some of the developmental defects associated with *lug*, *luh*, and *seu* mutants are caused by changes to pectin structure. This hypothesis is not without precedent, as previous work has shown that altering RG-I substitution in potato (*Solanum tuberosum*) plants causes a variety of developmental defects, including a reduction in shoot branching and a failure to form flowers, stolons, and tubers (Skjøt et al., 2002). As the effect of altering pectin structure is likely to be exacerbated during primary cell wall deposition, the LUG/LUH regulatory complex may also play a crucial role in elongating tissue.

MATERIALS AND METHODS

Plant Material and Growth Conditions

Wild-type Arabidopsis (*Arabidopsis thaliana*) plants were either Columbia (Col) or Columbia *erecta* (Col *er*). *luh-1* (seed stock no. CS91893), *luh-3* (seed stock no. SALK_107245C), *luh-4* (seed stock no. SALK_097509), *mum1-1* (seed stock no. CS91893), *mum2-1* (seed stock no. CS91893), and *mum2-2* (seed stock no. CS91893) mutant lines were obtained from the Arabidopsis Biological Resource Center. With the exception of *luh-1*, which is in the Col *er* background, all mutant lines are in the Col background (Western et al., 2001; Sitaraman et al., 2008; Stahle et al., 2009).

Plants were either grown on soil or on one-half-strength Murashige and Skoog medium in a growth room at 18°C or in a growth cabinet kept at 21°C under lights for 16 h.

Staining of Seed Mucilage

Seeds were gently shaken in distilled, deionized water for 2 h and then stained with 0.01% (w/v) ruthenium red for 2 h. Following a brief wash in distilled, deionized water, seeds were then viewed under bright-field optics. To stain seed sections, seeds were first embedded in Paraplast before generating 20-μm sections and staining for 5 min. Sections were viewed under bright-field optics using a Nikon SMZ800 dissecting microscope, and images were captured with a Nikon digital DS-U1 camera. To soften the cell wall, seeds were treated with 1 M Na_2CO_3, 50 mM EDTA, or 0.2% (w/v) ammonium oxalate for 2 h, rinsed twice in distilled, deionized water, and then stained with ruthenium red as outlined above.

RT-PCR

Developing seeds from 10-dpa siliques were placed in 10% glycerol and pressure applied to force embryo release. Following the manual collection of naked embryos and embryoless seeds (designated seed coats), RNA was isolated using an RNeasy RNA purification kit (Qiagen). Contaminating DNA was removed using DNA-free DNase (Ambion), and first-strand cDNA was synthesized with SuperScript III reverse transcriptase (Invitrogen) according to the manufacturer's instructions. All cDNAs were amplified using standard PCR conditions with primers described in Supplemental Table S2, and products were separated by gel electrophoresis. *ACTIN7* (*ACT7*; At5g09810) amplification involved 25 PCR cycles, whereas all other assays involved 30 PCR cycles. Due to near perfect sequence identity between *SLK1* and *SLK3*, PCR products were distinguished on the basis of *Bgl*II restriction digest. For qRT-PCR analysis, RNA from shoot, root, and seed tissue was used for first-

strand cDNA synthesis as described above. A Sensi-Mix dT kit (Quantace) was then used for real-time PCR analysis according to the manufacturer's instructions. PCR was performed in the presence of SYBR-Green on a Rotor-Gene 3000 Real-Time Cycler (Corbett Research) with *ACT7* as a housekeeping control.

Constructs

To generate *LUH* promoter constructs, 2.6 kb of genomic DNA upstream of the *LUH* coding sequence was amplified with high-fidelity Taq polymerase using oligonucleotides pLUH-F1/pLUH-R1, which incorporate *Pst*I and *Kpn*I restriction sites (Supplemental Table S2). The promoter fragment was then cloned into the *Pst*I/*Kpn*I sites of shuttle vector pMIGRO. LUH_{pro}*:LUG* and LUH_{pro}*:LUH* were made by placing the *LUG* and *LUH* coding sequences, which were generated by RT-PCR, downstream of the *LUH* promoter. Similarly, constructing LUH_{pro}*:MUM2* required amplification of the *MUM2* coding sequence, which was achieved by RT-PCR using primer combination MUM2-FK/MUM2-RB (Supplemental Table S2). *Kpn*I and *Bam*HI sites present in the primers were subsequently used to insert the cDNA downstream of the *LUH* promoter in pMIGRO. *Not*I-containing promoter-cDNA cassettes were then cloned into the binary vector pMLBART.

Binary vectors were introduced into *Agrobacterium tumefaciens* (GV3101) by electroporation and then transferred into plants using *Agrobacterium*-mediated floral dip (Clough and Bent, 1998). Transformants were identified following BASTA treatment.

Histology and Microscopy

Siliques harvested at 6, 9, and 12 dpa were fixed in 2.5% glutaraldehyde overnight at 4°C and then treated with 1% osmium tetroxide. Tissue was passed through a graded ethanol series and subsequently embedded in LR-White resin. For histological analysis, 2-μm sections were stained with toluidine blue and examined under bright-field optics using a DM2500 Leica compound light microscope. For immunolabeling, 80-nm sections were processed according to established procedures (Burton et al., 2006). Grids were initially exposed to a 1:50 dilution of primary antibody (JIM5 and JIM7; Plant Probes), washed, and then treated with secondary antibody conjugated to 18-nm gold particles (Jackson ImmunoResearch). Samples were washed, treated with 2% aqueous uranyl acetate, and viewed by transmission electron microscopy as described previously (Burton et al., 2006).

SEM of whole seeds was performed with an FEI Quanta environmental SEM device at room temperature using an accelerating voltage of 12.5 kV.

Histochemical Analysis

The LUH_{pro}*::GUS* construct has been described previously (Macquet et al., 2007b; Stahle et al., 2009). Siliques at 3, 6, and 9 dpa were sliced open, vacuum infiltrated for 1 h, and incubated overnight in 50 mM phosphate buffer containing 2 mM 5-bromo-4-chloro-3-indolyl-β-glucuronic acid and a mixture of 1 mM potassium ferricyanide and ferrocyanide at 37°C. Siliques were washed, fixed in formaldehyde-acetic acid, and passed through a graded ethanol series. Seeds were then placed in Hoyer's solution before being viewed under differential interference contrast optics.

Linkage Analysis of Mucilage

Seed mucilage was extracted using an acid/alkali procedure (Macquet et al., 2007b) with minor modifications. Seeds were shaken vigorously (900 rpm) in 50 mM HCl at 85°C for 30 min, rinsed with distilled, deionized water, and then shaken again in 1 M NaOH containing 10 mg mL^{-1} $NaBH_4$ at room temperature for 40 min. Seeds were then rinsed several times with distilled, deionized water. The acid and alkali fractions were neutralized and dialyzed extensively against deionized water for 24 h before being freeze dried.

Isolated mucilage polysaccharide was carboxyl reduced and subsequently methylated according to established methods (Kim and Carpita, 1992; Sims and Bacic, 1995). For GC-MS, samples were resuspended in dichloromethane and subsequently loaded onto a BPX70 column for analysis as described previously (Lau and Bacic, 1993).

Polysaccharide content was estimated from the methylation data essentially as described by Shea et al. (1989) and Zhu et al. (2005).

Supplemental Data

The following materials are available in the online version of this article.

Supplemental Figure S1. SEM of wild-type and mutant seeds.

Supplemental Figure S2. Mucilage release from *luh* mutants following chemical treatment.

Supplemental Figure S3. RT-PCR analysis using wild-type and *luh* mutant seed tissue.

Supplemental Figure S4. Mucilage release from seed coats following acid/alkali treatment.

Supplemental Figure S5. Comparison of developing wild-type, *luh*, and *luh;lug*/+ mutant seed coats.

Supplemental Table S1. Linkage analysis of alkali-extracted mucilage from wild-type, mutant, and transgenic lines.

Supplemental Table S2. Primer sequences used for RT-PCR, real-time PCR, and cloning.

ACKNOWLEDGMENTS

We thank Nicole Crequer for help with root growth assays, Roger Curtain for technical assistance with the environmental SEM, Cherie Walsh for technical assistance with the GC-MS, and members of the Golz and Plant Cell Biology Research Centre laboratories for critically reading the manuscript. We also thank George Haughn for pointing out the similarities between the *mum1* and *luh* phenotypes.

Received January 16, 2011; accepted March 12, 2011; published March 14, 2011.

LITERATURE CITED

Arsovski AA, Popma TM, Haughn GW, Carpita NC, McCann MC, Western TL (2009) AtBXL1 encodes a bifunctional β-D-xylosidase/α-L-arabinofuranosidase required for pectic arabinan modification in Arabidopsis mucilage secretory cells. Plant Physiol **150:** 1219–1234

Azadi P, O'Neill MA, Bergmann C, Darvill AG, Albersheim P (1995) The backbone of the pectic polysaccharide rhamnogalacturonan I is cleaved by an endohydrolase and an endolyase. Glycobiology **5:** 783–789

Bao F, Azhakanandam S, Franks RG (2010) SEUSS and SEUSS-LIKE transcriptional adaptors regulate floral and embryonic development in Arabidopsis. Plant Physiol **152:** 821–836

Beeckman T, De Rycke R, Viane R, Inze D (2000) Histological study of seed coat development in *Arabidopsis thaliana*. J Plant Res **113:** 139–148

Boesewinkel FD, Bouman F (1995) The seed: structure and function. *In* J Kigel, G Galili, eds, Seed Development and Germination. Marcel Dekker, New York, pp 1–24

Bowman JL, Smyth DR, Meyerowitz EM (1989) Genes directing flower development in *Arabidopsis*. Plant Cell **1:** 37–52

Burton RA, Wilson SM, Hrmova M, Harvey AJ, Shirley NJ, Medhurst A, Stone BA, Newbigin EJ, Bacic A, Fincher GB (2006) Cellulose synthase-like CslF genes mediate the synthesis of cell wall (1,3;1,4)-β-D-glucans. Science **311:** 1940–1942

Byrne ME, Barley R, Curtis M, Arroyo JM, Dunham M, Hudson A, Martienssen RA (2000) *Asymmetric leaves1* mediates leaf patterning and stem cell function in *Arabidopsis*. Nature **408:** 967–971

Caffall KH, Pattathil S, Phillips SE, Hahn MG, Mohnen D (2009) *Arabidopsis thaliana* T-DNA mutants implicate GAUT genes in the biosynthesis of pectin and xylan in cell walls and seed testa. Mol Plant **2:** 1000–1014

Clough SJ, Bent AF (1998) Floral dip: a simplified method for *Agrobacterium*-mediated transformation of *Arabidopsis thaliana*. Plant J **16:** 735–743

Coutinho PM, Henrissat B (1999) Carbohydrate-active enzymes: an integrated database approach. *In* HJ Gilbert, G Davies, B Henrissat, B Svensson, eds, Recent Advances in Carbohydrate Bioengineering. Royal Society of Chemistry, Cambridge, UK, pp 3–12

Dean GH, Zheng H, Tewari J, Huang J, Young DS, Hwang YT, Western TL, Carpita NC, McCann MC, Mansfield SD, et al (2007) The *Arabi-*

dopsis MUM2 gene encodes a β-galactosidase required for the production of seed coat mucilage with correct hydration properties. Plant Cell **19:** 4007–4021

De Veau EJI, Gross KC, Huber DJ, Watada AE (1993) Degradation and solubilization of pectin by β-galactosidases purified from avocado mesocarp. Physiol Plant **87:** 279–285

Gutterman Y, Shemtov S (1996) Structure and function of the mucilaginous seed coats of *Plantago coronopus* inhabiting the Negev desert of Israel. Isr J Plant Sci **44:** 125–133

Johnson CS, Kolevski B, Smyth DR (2002) *TRANSPARENT TESTA GLABRA2*, a trichome and seed coat development gene of *Arabidopsis*, encodes a WRKY transcription factor. Plant Cell **14:** 1359–1375

Kim JB, Carpita NC (1992) Changes in esterification of the uronic acid groups of cell wall polysaccharides during elongation of maize coleoptiles. Plant Physiol **98:** 646–653

Knox JP, Linstead PJ, King J, Cooper C, Roberts K (1990) Pectin esterification is spatially regulated both within cell walls and between developing tissue of root apices. Planta **181:** 512–521

Koornneef M (1981) The complex syndrome of *ttg* mutants. Arabidopsis Inf Serv **18:** 45–51

Lau E, Bacic A (1993) Capillary gas chromatography of partially methylated alditol acetates on a high-polarity, cross-liked, fused-silica BPX70 column. J Chromatogr **637:** 100–103

Leon-Kloosterziel KM, Keijzer CJ, Koornneef M (1994) A seed shape mutant of *Arabidopsis* that is affected in integument development. Plant Cell **6:** 385–392

Li SF, Milliken ON, Pham H, Seyit R, Napoli R, Preston J, Koltunow AM, Parish RW (2009) The *Arabidopsis* MYB5 transcription factor regulates mucilage synthesis, seed coat development, and trichome morphogenesis. Plant Cell **21:** 72–89

Liu Z, Karmarkar V (2008) Groucho/Tup1 family co-repressors in plant development. Trends Plant Sci **13:** 137–144

Macquet A, Ralet MC, Kronenberger J, Marion-Poll A, North HM (2007a) In situ, chemical and macromolecular study of the composition of *Arabidopsis thaliana* seed coat mucilage. Plant Cell Physiol **48:** 984–999

Macquet A, Ralet MC, Loudet O, Kronenberger J, Mouille G, Marion-Poll A, North HM (2007b) A naturally occurring mutation in an *Arabidopsis* accession affects a β-D-galactosidase that increases the hydrophilic potential of rhamnogalacturonan I in seed mucilage. Plant Cell **19:** 3990–4006

Mohnen D (2008) Pectin structure and biosynthesis. Curr Opin Plant Biol **11:** 266–277

Mutter M, Colquhoun IJ, Beldman G, Schols HA, Bakx EJ, Voragen AG (1998) Characterization of recombinant rhamnogalacturonan α-L-rhamnopyranosyl-(1,4)-α-D-galactopyranosyluronide lyase from *Aspergillus aculeatus*: an enzyme that fragments rhamnogalacturonan I regions of pectin. Plant Physiol **117:** 141–152

Naran R, Pierce ML, Mort AJ (2007) Detection and identification of rhamnogalacturonan lyase activity in intercellular spaces of expanding cotton cotyledons. Plant J **50:** 95–107

Nesi N, Debeaujon I, Jond C, Pelletier G, Caboche M, Lepiniec L (2000) The *TT8* gene encodes a basic helix-loop-helix domain protein required for expression of *DFR* and *BAN* genes in *Arabidopsis* siliques. Plant Cell **12:** 1863–1878

Oka T, Nemoto T, Jigami Y (2007) Functional analysis of *Arabidopsis thaliana* RHM2/MUM4, a multidomain protein involved in UDP-D-glucose to UDP-L-rhamnose conversion. J Biol Chem **282:** 5389–5403

Penfield S, Meissner RC, Shoue DA, Carpita NC, Bevan MW (2001) MYB61 is required for mucilage deposition and extrusion in the *Arabidopsis* seed coat. Plant Cell **13:** 2777–2791

Rautengarten C, Usadel B, Neumetzler L, Hartmann J, Büssis D, Altmann T (2008) A subtilisin-like serine protease essential for mucilage release from *Arabidopsis* seed coats. Plant J **54:** 466–480

Schols HA, Voragen AGJ (1996) Complex pectins: structure elucidation using enzymes. *In* J Visser, AGJ Voragen, eds, Pectins and Pectinases. Elsevier Science, Amsterdam, pp 3–19

Shea EM, Gibeaut DM, Carpita NC (1989) Structural analysis of the cell walls regenerated by carrot protoplasts. Planta **179:** 293–308

Sims IM, Bacic A (1995) Extracellular polysaccharides from suspension cultures of Nicotiana plumbaginifolia. Phytochemistry **38:** 1397–1405

Sitaraman J, Bui M, Liu Z (2008) LEUNIG_HOMOLOG and LEUNIG perform partially redundant functions during Arabidopsis embryo and floral development. Plant Physiol **147:** 672–681

Skjøt M, Pauly M, Bush MS, Borkhardt B, McCann MC, Ulvskov P (2002) Direct interference with rhamnogalacturonan I biosynthesis in Golgi vesicles. Plant Physiol **129:** 95–102

Sridhar VV, Surendrarao A, Gonzalez D, Conlan RS, Liu Z (2004) Transcriptional repression of target genes by LEUNIG and SEUSS, two interacting regulatory proteins for *Arabidopsis* flower development. Proc Natl Acad Sci USA **101:** 11494–11499

Stahle MI, Kuehlich J, Staron L, von Arnim AG, Golz JF (2009) YABBYs and the transcriptional corepressors LEUNIG and LEUNIG_HOMOLOG maintain leaf polarity and meristem activity in *Arabidopsis*. Plant Cell **21:** 3105–3118

Usadel B, Kuschinsky AM, Rosso MG, Eckermann N, Pauly M (2004) RHM2 is involved in mucilage pectin synthesis and is required for the development of the seed coat in Arabidopsis. Plant Physiol **134:** 286–295

Western TL (2006) Changing spaces: the *Arabidopsis* mucilage secretory cells as a novel system to dissect cell wall production in differentiating cells. Can J Bot **84:** 622–630

Western TL, Burn J, Tan WL, Skinner DJ, Martin-McCaffrey L, Moffatt BA, Haughn GW (2001) Isolation and characterization of mutants defective in seed coat mucilage secretory cell development in Arabidopsis. Plant Physiol **127:** 998–1011

Western TL, Skinner DJ, Haughn GW (2000) Differentiation of mucilage secretory cells of the Arabidopsis seed coat. Plant Physiol **122:** 345–356

Western TL, Young DS, Dean GH, Tan WL, Samuels AL, Haughn GW (2004) *MUCILAGE-MODIFIED4* encodes a putative pectin biosynthetic enzyme developmentally regulated by APETALA2, TRANSPARENT TESTA GLABRA1, and GLABRA2 in the Arabidopsis seed coat. Plant Physiol **134:** 296–306

Willats WG, Limberg G, Buchholt HC, van Alebeek GJ, Benen J, Christensen TM, Visser J, Voragen A, Mikkelsen JD, Knox JP (2000) Analysis of pectic epitopes recognised by hybridoma and phage display monoclonal antibodies using defined oligosaccharides, polysaccharides, and enzymatic degradation. Carbohydr Res **327:** 309–320

Willats WG, McCartney L, Knox JP (2001) *In-situ* analysis of pectic polysaccharides in seed mucilage and at the root surface of *Arabidopsis thaliana*. Planta **213:** 37–44

Windsor JB, Symonds VV, Mendenhall J, Lloyd AM (2000) *Arabidopsis* seed coat development: morphological differentiation of the outer integument. Plant J **22:** 483–493

Zhang F, Gonzalez A, Zhao M, Payne CT, Lloyd A (2003) A network of redundant bHLH proteins functions in all TTG1-dependent pathways of *Arabidopsis*. Development **130:** 4859–4869

Zhu Y, Pettolino F, Mau SL, Bacic A (2005) Characterization of cell wall polysaccharides from the medicinal plant *Panax notoginseng*. Phytochemistry **66:** 1067–1076